

# Patterned growth on GaAs (311)A substrates: Dependence on mesa misalignment and sidewall slope and its application to coupled wire-dot arrays

Jörg Fricke,<sup>a)</sup> Richard Nötzel, Uwe Jahn, Hans-Peter Schönherr, Lutz Däweritz, and Klaus H. Ploog

*Paul-Drude-Institut für Festkörperelektronik, Hausvogteiplatz 5-7, D-10117 Berlin, Germany*

(Received 9 October 1998; accepted for publication 23 December 1998)

During molecular beam epitaxy of (AlGa)As on patterned GaAs (311)A substrates, mesa stripes along [01-1] develop a fast-growing sidewall with a smooth, unfacetted, convex surface profile which has been utilized for the formation of lateral quantum wires. In the present study this growth mechanism is found to be strongly sensitive, both on the misalignment of the mesa stripes from the [01-1] direction as well as on the sidewall slope. For wet chemical etching which produces a 50° steep sidewall of the starting mesa stripe along [01-1], the formation of the convex surface profile is not affected for a misalignment smaller than 20°. Above 20°, the selectivity of growth monotonically decreases and the surface profile continuously develops into that of the slow growing concave sidewall along the perpendicular [-233] direction for misalignment larger than 50°. In contrast, for reactive ion etched vertical sidewalls, almost no growth occurs for [01-1]-oriented mesa stripes while the evolution of the fast growing sidewall is recovered for misaligned mesa stripes. This behavior, which is qualitatively related to the bond configuration of the starting side facets, thus provides a unique parameter to control the selectivity of growth on patterned GaAs (311)A substrates, which is utilized for the formation of coupled wire-dot structures. © 1999 American Institute of Physics. [S0021-8979(99)00607-6]

## I. INTRODUCTION

Patterned growth has proven to be a powerful technique for the formation of low-dimensional semiconductor structures, i.e., quantum wires and quantum dots as well as the monolithic integration of devices. During the last decade the formation of quantum wires and quantum dots in patterned growth has been mainly concentrated on the formation of V-groove<sup>1,2</sup> and ridge-type<sup>3-7</sup> structures on low-index GaAs (100) and (111) substrates. By growing GaAs/(AlGa)As heterostructures, the plane-type depending migration length of adatoms, being larger on the sidewalls, leads to the evolution of slow-growing side facets due to migration of adatoms on top of narrow ridges or in the bottom of V grooves to produce the laterally confined nanostructures. The aim of all these activities is to find the optimum growth conditions and pattern configuration which result in high shape uniformity of the quantum wires and quantum dots, high density, strong lateral confinement, and compatibility to further processing steps. The growth of dense arrays of V-groove or ridge-type structures, however, suffers from increased size fluctuations and reduced growth selectivity, i.e., lateral confinement of carriers due to fast planarization of the growth front,<sup>8</sup> whereas isolated deep V grooves or ridges are difficult to process by following lithographic steps. Moreover, the formation of extended side facets of high uniformity is very sensitive to small misalignment of the pattern easily generating strong size fluctuations giving rise to irregular dot-like emission patterns.<sup>9</sup>

To overcome these problems we investigate the growth of GaAs/(AlGa)As heterostructures on patterned GaAs (311)A substrates by molecular beam epitaxy (MBE), which has recently revealed growth mechanisms for the selective growth of low-dimensional nanostructures with improved structural and electronic properties.<sup>10,11</sup> Mesa stripes oriented along the [01-1] direction prepared by wet chemical etching develop a fast-growing sidewall in the sector towards the next (100) plane with a very smooth, unfacetted, convex surface profile which relies on the migration of adatoms from both sides, the mesa bottom, and mesa top towards the sidewall. On the opposite sidewall a slow growing (111)A side facet with the common concave surface profile evolves due to migration of adatoms away from the sidewall. Mesa stripes oriented along the perpendicular [2-3-3] direction develop ridge-type structures by forming symmetric slow-growing side facets on both sides, similar to the case of the low-index (100) and (111) planes.<sup>12</sup> Intersecting these two sidewalls in periodic square-shaped hole patterns results in triangular-shaped dot-like structures between the holes on the original substrate surface.<sup>13</sup> The formation of the fast-growing sidewall at shallow mesa stripes with 10–20 nm height results in lateral, quasiplanar quantum wires with excellent optical properties.<sup>14</sup> The wires have been stacked on submicron gratings in dense, three-dimensional arrays without degradation of the uniformity and lateral confinement energies exceeding 200 meV.<sup>11</sup>

In this article we demonstrate the influence of the misalignment of the mesa stripe from the [01-1] direction as well as of the sidewall slope on the selectivity of growth, i.e.,

<sup>a)</sup>Electronic mail: fricke@pdi-berlin.de

on the formation of sidewall quantum wires on patterned GaAs (311)A substrates. For wet chemically etched mesas, which exhibit a  $50^\circ$  steep sidewall along [01-1], the selectivity of growth is almost not affected for a misalignment as large as  $20^\circ$ , thus making the wire formation highly insensitive to small deviations of the mesa stripe from the [01-1] direction. Above  $20^\circ$  misalignment the selectivity of the fast-growing sidewall monotonically reduces and the surface profile develops into that of the slow-growing sidewall along the perpendicular [2-3-3] direction for misalignment larger than  $50^\circ$ . In contrast, on vertical sidewalls prepared by reactive ion etching almost no growth occurs for mesa stripes along [01-1]. The evolution of the fast-growing sidewall is, however, recovered for misaligned mesa stripes. This behavior, which is qualitatively explained by the bond configuration of the starting facets thus provides a unique means to control the selectivity of growth on patterned GaAs (311)A substrates, which is utilized for the formation of coupled wire-dot structures.

## II. SAMPLE PREPARATION AND EXPERIMENTAL SETUP

An AZ5214 photoresist mask and standard optical lithography were used to define  $10\ \mu\text{m}$  wide mesa stripes on the GaAs (311)A substrate which are oriented along [01-1] as well as progressively misaligned by steps of  $10^\circ$ . For wet chemical etching the  $\text{H}_2\text{SO}_4:\text{H}_2\text{O}_2:\text{H}_2\text{O}$  (1:8:40) etch solution was used. Reactive ion etching (RIE) was carried out in a standard parallel-plate reactor, using a  $\text{Cl}_2/\text{N}_2$  plasma for 500 nm deep vertical sidewalls and a pure  $\text{CF}_4$  plasma, in the case followed by a short  $\text{Cl}_2$  etch step for shallow mesas of 15–20 nm height. Both wet chemical and reactive ion etching produced the same smooth surfaces as confirmed by scanning electron microscopy (SEM). After etching, the samples were cleaned in concentrated  $\text{H}_2\text{SO}_4$  and rinsed in deionized water. The native oxide was removed in the MBE preparation chamber by atomic hydrogen before the samples were loaded into the growth chamber. For studying the growth mode on the 500 nm deep etched mesas, a 50 nm thick GaAs buffer layer was grown which was followed by 100 nm  $\text{Al}_{0.5}\text{Ga}_{0.5}\text{As}$ , a multilayer structure of three times 300 nm GaAs/100 nm  $\text{Al}_{0.5}\text{Ga}_{0.5}\text{As}$ , a 6 nm thick GaAs quantum-well layer, 100 nm  $\text{Al}_{0.5}\text{Ga}_{0.5}\text{As}$ , and finally, a 20 nm thick GaAs cap. The layer sequence on the shallow mesas for the formation of sidewall quantum wires comprised a 50 nm thick GaAs buffer layer, a 3 nm thick GaAs quantum-well layer embedded between two 50 nm thick  $\text{Al}_{0.5}\text{Ga}_{0.5}\text{As}$  lower and upper barrier layers, and a 20 nm thick GaAs cap. The growth temperature was  $620^\circ\text{C}$  and the growth rates for GaAs and  $\text{Al}_{0.5}\text{Ga}_{0.5}\text{As}$  were 0.5 and  $1\ \mu\text{m}/\text{h}$ . During growth the substrates were rotated by 6 rpm to avoid any shadowing effects. The structural and optical properties have been investigated by scanning electron microscopy and cathodoluminescence (CL) spectroscopy. For the cross-sectional SEM investigations, the samples were sawed perpendicular to the mesa stripes and stain etched in  $\text{NH}_4:\text{H}_2\text{O}_2:\text{H}_2\text{O}$  (1:30:200) for 5 s.

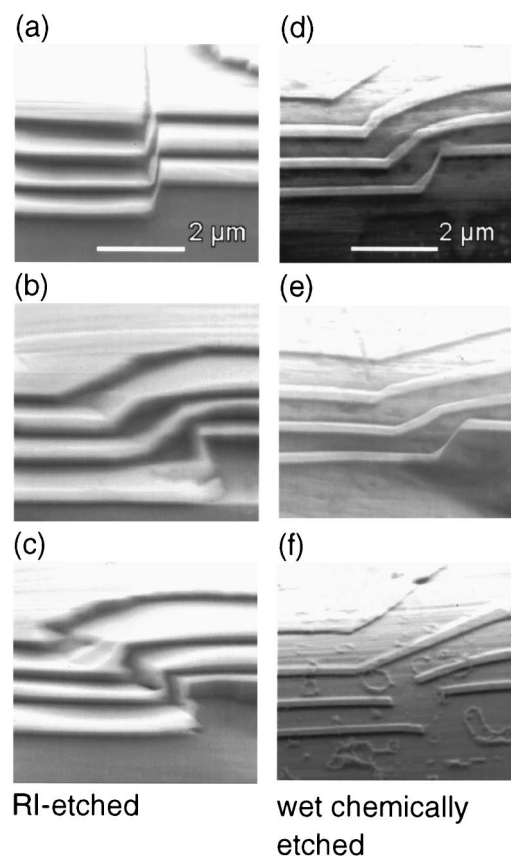


FIG. 1. Cross-sectional SEM images of RI-etched vertical mesa sidewalls on patterned GaAs (311)A substrates in the sector towards the next (100) plane after overgrowth. (a) Oriented along [01-1], (b) misaligned by  $30^\circ$ , and (c) misaligned by  $50^\circ$  from [01-1]. (d)–(f) Corresponding SEM images of wet chemically etched sidewalls with  $50^\circ$  slope.

## III. RESULTS AND DISCUSSION

Figures 1(a)–1(c) show the cross-sectional SEM images of the GaAs/(AlGa)As multilayer structure at the RI-etched vertical sidewalls for a misalignment of (a)  $0^\circ$ , (b)  $30^\circ$ , and (c)  $50^\circ$ . The corresponding SEM images for the wet chemically etched tilted sidewalls are depicted in Figs. 1(d)–1(f). The dark contrast is due to GaAs and the lighter one due to (AlGa)As. The poor contrast in some of the images is caused by the necessity of sawing the samples where no perpendicular cleavage plane is available, which even can break off parts of the layers. The close spacing between the (AlGa)As marker layers in Fig. 1(a) indicates negligible growth of GaAs on the vertical sidewall along [01-1] without visible accumulation of material on the mesa top and bottom close to the sidewall. Increasing the misalignment to  $\pm 30^\circ$  [Fig. 1(b)], in contrast, results in very effective lateral growth on the vertical sidewall. The results for the misaligned mesas are always identical with respect to clockwise (+) or counterclockwise (-) misalignment in agreement with the crystal symmetry. After preferential filling of the bottom step edge, the typical convex shape of the fast-growing sidewall develops after size reduction of a fast-growing side facet close to the next (100) plane. For the misalignment of  $\pm 50^\circ$  in Fig. 1(c) the growth rate on the vertical sidewall decreases to a value comparable to that on the (311)A surface, evidenced

by the almost uniform layer thickness across the sidewall. The evolution of the growth front on the wet chemically etched sidewalls with  $50^\circ$  slope [Figs. 1(d)–1(f)], on the other hand, is characterized by the formation of the fast-growing convex sidewall already at  $0^\circ$  misalignment with a monotonously decreasing growth rate for increasing misalignment of  $30^\circ$  reaching an almost uniform layer thickness at  $50^\circ$ . Independent of the mesa misalignment, the surface morphology remains very smooth without the evolution of microfacets. Only the RI-etched vertical sidewall along [01-1] with negligible growth rate shows some roughening, typical for slow-growing  $\{111\}$  planes.

In general, the growth on patterned substrates is governed by the migration of adatoms among the competing growth planes from slow-growing facets with a larger surface migration length to fast-growing facets with the smaller surface migration length. The surface migration lengths on the different growth planes in turn are determined by the specific atomic configuration, i.e., surface reconstruction, and step density of the sidewalls or facets. Both the reconstruction and the step structure of a surface are, however, related to the structure of the ideal surface, corresponding to the truncation through the bulk structure. Therefore, as a first step towards a structural interpretation of the sidewall growth, the configuration of the ideal surfaces of the different patterned sidewalls depending on misalignment and slope are taken into account although it is known that particularly for high-index planes the true microscopic surface structure can be indeed very sophisticated.<sup>15</sup>

The atomic structure of surfaces derived from the bulk crystal is characterized by the tetrahedral configuration of the four nearest neighbors. For our discussion the atomic configuration of arbitrary surfaces is described by the tilt alone, and not the orientation of the tetrahedrons with respect to the (1-1-1) and (100) planes, which relates to the character of a specific surface and thus the migration length of adatoms, i.e., their incorporation probability. In Figs. 2(a)–2(h) the top view of the atomic planes with different orientations corresponding to the various side facets are compared with that of the singular (1-1-1) and (100) planes. The tetrahedron arrangement of the (1-1-1) and (100) planes [Figs. 2(a) and 2(b)] most differ in that one tetrahedron plane is parallel to the (1-1-1) plane while all four tetrahedron planes have the largest possible angle with the surface if we look at the (100) plane. Therefore, for the (100) plane, two bonds per atom are directed towards the surface which enhance the adatom incorporation (or reduce the surface migration length) and drive the As dimerization into the various surface reconstructions, depending on the growth conditions. On the other hand, for the (1-1-1) plane only a single bond per atom is directed towards the surface, indicating a reduced adatom incorporation probability. In fact, in patterned growth on GaAs (100) substrates, mesa stripes oriented along the [01-1] direction develop slow growing (111)A side facets consistent with the larger surface migration length of adatoms on the  $\{111\}$  planes compared to that on  $\{100\}$  planes.

Based on the atomic configuration of the  $\{100\}$  and  $\{111\}$  planes and their relationship with the surface migration length, a direct comparison of the atomic configuration of the

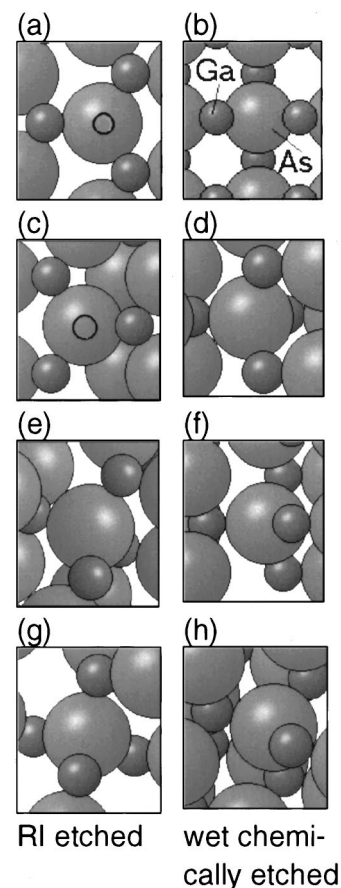


FIG. 2. Top view of the bulk Ga–As tetrahedron for the (a) (1-1-1), (b) (100), (c) (2-3-3), (d) (3-1-1), (e), (2-5-1), (f) (-2-5-2), (g) (2-71), and (h) (8-63) planes representing the various side facets of the mesa sidewalls obtained on patterned GaAs (311)A substrates in dependence of the misalignment and sidewall slope.

as-etched sidewalls in Fig. 1 for different slope, but the same misalignment, can account for the observed growth behavior. This simple relation of the atomic configuration of the starting surface to the growth selectivity can be applied due to the smooth as-etched surfaces and the absence of microfacets during growth. A brief compilation of the following discussion is given in Table I. The Miller indices are calculated from the misalignment and sidewall slope, determined from SEM. The atomic configuration of the RIE-patterned vertical sidewall along [01-1] [Fig. 1(a)], i.e., (2-3-3) plane, is shown in Fig. 2(c). The arrangement of the tetrahedron is very close to that of the (1-1-1) plane in Fig. 2(a). On the other hand, for the wet chemically etched sidewall with  $50^\circ$  slope, corresponding to the (3-1-1) plane shown in Fig. 2(d), the appearance of the tetrahedron is close to that of the (100) surface [Fig. 2(b)]. This is consistent with the observation that for vertical sidewalls the growth is terminated close to the next slow-growing (111) plane inclined by  $80^\circ$  having a growth rate smaller than that of the (311) surface, while for the tilted wet chemically etched sidewall there is no slower growing plane in the remaining open sector. Starting from a facet similar to the next (100) plane the fast-growing sidewall can develop. This shows that for realizing a fast-growing sidewall it is not only important to find the correct

TABLE I. Miller indices and growth evolution of the RI-etched (vertical) and wet chemically etched (tilted) sidewalls in dependence of the mesa misalignment.

Misalignment (°)	RI-etched (vertical sidewall)			Wet chemically etched (tilted sidewall)		
	Indices	See Fig.	Growth rate	Indices	See Fig.	Growth rate
0	(2-3-3)	1(a), 2(c)	Minimal	(3-1-1)	1(d), 2(d)	High
30	(2-5-1)	1(b), 2(e)	High	(-2-5-2)	1(e), 2(f)	Medium
50	(2-71)	1(c), 2(g)	Medium	(8-63)	1(f), 2(h)	Medium

surface orientation and mesa alignment, but also the suitable opening of the free sector defined by the sidewall slope of the mesa stripe.

Coming back to the vertical sidewall in Fig. 1(b), which is misaligned by 30°, the tilt of the tetrahedron of the corresponding (2-5-1) plane shown in Fig. 2(e) is very similar to that of the (3-1-1) plane having the character of (100) planes. Although microscopically the (2-5-1) plane is composed of different low-index planes it is, therefore, understood that by rotating the vertical mesa sidewall away from the [01-1] direction, that is, away from the slow-growing (111) plane, the configuration of a fast-growing sidewall returns, which is observed in the experiment. The 30° misaligned wet chemically etched sidewall shown in Fig. 1(e), which corresponds to the (-2-5-2) plane in Fig. 2(f), undergoes a continuous rotation away from the fast-growing (100) configuration consistent with the reduced growth rate. The absence of a nearby slow-growing plane with (111) character in the open sector, which could terminate the growth, is fulfilled for the (3-1-1), (2-5-1), and (-2-5-2) planes. With further increase of the mesa misalignment to ±50° [Figs. 1(c) and 1(f)], a very similar growth behavior is observed for RI and wet chemical etching with an almost uniform layer thickness across the sidewall due to the transition from the fast-growing sidewall along [01-1] to the slow-growing sidewall along [2-3-3]. This is consistent with the tilt of the tetrahedrons for both the vertical RI-etched and tilted wet chemically etched sidewalls corresponding to (2-71) [Fig. 2(g)] and (8-63) [Fig. 2(h)] planes being almost intermediate between the fast-growing (100) and the slow-growing (111) plane with respect to the (311) surface.

The continuous changeover from the fast-growing to the slow-growing sidewall for wet chemically etched sidewalls in dependence of the misalignment is confirmed by spatially resolved CL measurements of the quantum-well layer inset in the structure depicted in Fig. 1. Figure 3 shows the peak position of the quantum-well layer at the sidewall (solid line) and that in the flat area on the mesa top (dashed line) for different misalignment. The insets image the evolution of the growth front determined from SEM. Below 40°–50° the CL peak position at the sidewall is redshifted compared to that in the flat area, indicating the thicker quantum-well layer at the fast-growing sidewall. Between 40° and 50° the CL peak position at the sidewall approaches that in the flat area due to the changeover from the fast- to the slow-growing sidewall with uniform layer thickness and, consequently, further shifts to higher energy up to the mesa alignment along [2-3-3]. It is surprising that the CL peak position of the quantum-well layer at the sidewall remains almost constant for misalign-

ment below 20°. This demonstrates that the selectivity of growth at the fast-growing sidewall is remarkably insensitive to small misalignment, which supports the formation of uniform quantum wires at shallow mesa stripes where small undulations of the sidewall can hardly be avoided by standard lithographic techniques.

#### IV. FORMATION OF COUPLED WIRE-DOT ARRAYS

The results obtained on the selectivity of growth on misaligned mesa stripes are directly applied to the formation of coupled wire-dot structures. The idea is to create a dot-like structure with locally thicker layer thickness, i.e., smaller band-gap energy at the corner of two intersecting mesas which are symmetrically inclined from the [01-1] azimuth to connect a wire structure with lower growth selectivity, i.e., larger band-gap energy. This is demonstrated by fabricating a zigzag pattern with 4.5 μm long sidewalls, alternatingly misaligned by + or -30° with respect to the [0 1 -1] direction. The sidewall is etched to a depth of 15 nm for which a combined CF<sub>4</sub> and Cl<sub>2</sub>/N<sub>2</sub> RI-etching process produces a nonvertical slope.

The formation of the coupled wire-dot structure is investigated by spectrally and spatially resolved CL spectroscopy. The overview spectrum shown in Fig. 4 is taken at 4 K from a 3 × 3 μm<sup>2</sup> large scan field centered at one corner of the mesa structure. Four peaks at 1.735, 1.710, 1.668, and 1.644 eV are clearly resolved. Their spatial origin is revealed by the corresponding CL images detected at the corresponding peak energies [Figs. 5(a)–5(d)]. Starting from the high-

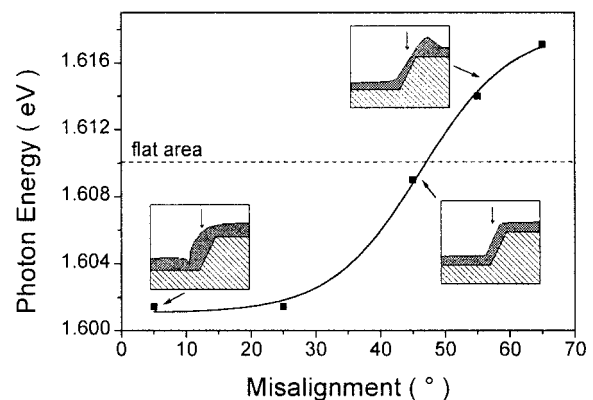


FIG. 3. CL peak position of the quantum-well emission at the mesa sidewall in dependence of the misalignment from the [01-1] direction for wet chemically etched 500 nm deep tilted sidewalls. The inset indicates the schematic cross section determined from SEM with the arrows indicating the excitation position.

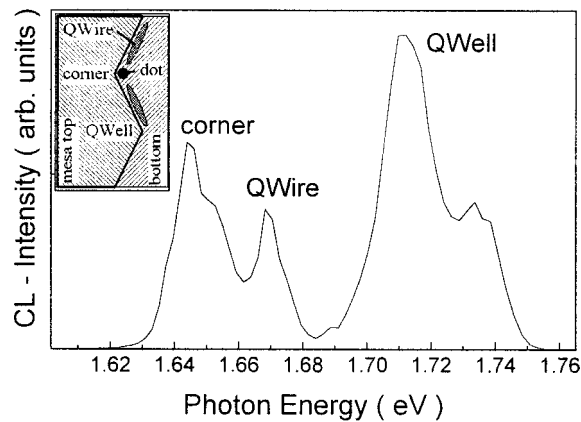


FIG. 4. CL spectrum taken at 4 K from a  $3 \times 3 \mu\text{m}$  large scan field centered at the corner of the zigzag pattern etched to a depth of 15 nm. The inset indicates the spatial origin of the emission from the quantum well in the flat area (QWell), the quantum wire (QWire) at the inclined sidewalls, and the dot at the corner.

energy side of the spectrum, the peak at 1.735 eV [Fig. 5(a)] originates from the thinner areas in the vicinity of the sidewall due to the migration of adatoms towards the sidewall forming the wires. Due to the spatial resolution, the drop in intensity of this emission at the sidewall in the wire region is not resolved in this image. The peak at 1.710 eV [Fig. 5(b)] is from the emission of the quantum well in the flat areas of the mesa structure. The wire structure at the misaligned sidewall with reduced growth selectivity compared to exactly [01-1]-oriented sidewalls is revealed in the CL image detected at 1.668 eV in Fig. 5(c), while the emission at the lowest energy at 1.644 eV [Fig. 5(d)] originates from the corner of the sidewalls forming the dot-like structure with the locally largest layer thickness. The weak shoulder at 1.652 eV is attributed to the transition region from the side-

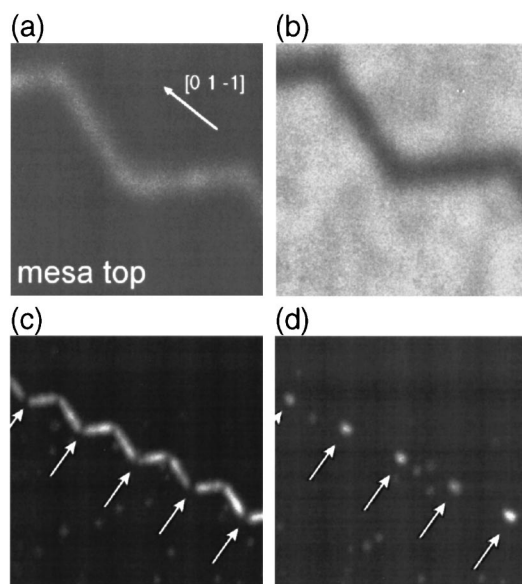


FIG. 5. CL images detected at the peak energies of the spectrum of Fig. 4 at (a) 1.735 eV, (b) 1.710 eV, (c) 1.668 eV, and (d) 1.644 eV. The scan field is (a),(b)  $10 \times 10 \mu\text{m}^2$  and (c),(d)  $40 \times 40 \mu\text{m}^2$ . The arrows indicate the position of the dot structure at the corner of the sidewalls.

wall wire structure to the dot structure at the corner. At present, however, it is not clear why the dot-like structures are found predominantly in the corners and not on the tips of the zigzag pattern although at both positions the emission from the sidewall wires is disconnected. Finally, it should be noted that in the present case of coupled wire-dot formation, which is based on lateral transport of material from the mesa top and bottom to the sidewall, there is no apparent depletion of material, i.e., an additional energy barrier between the wire and the dot which is usually encountered for ridge-type structures on patterned GaAs (100) substrates.<sup>16,17</sup> The exciton transfer from the wires into the dots is revealed in a distinct shape of the dot emission extending into the wire regions in temperature dependent CL mapping (not shown here). This might be advantageous in addressing the dots electrically through the connecting wires for applications like memory devices or shift registers.

## V. CONCLUSIONS

In summary, we have investigated the growth of GaAs/(AlGa)As heterostructures on patterned GaAs (311)A substrates by molecular beam epitaxy in dependence of the mesa misalignment and sidewall slope. Wet chemically etched mesa sidewalls along [01-1] with a slope of  $50^\circ$  reveal the evolution of a fast-growing, unafaceted, convex sidewall reported previously. Cross-sectional electron microscopy reveals the evolution of the sidewall to be almost unaffected for a misalignment smaller than  $20^\circ$ , which explains that the uniformity of sidewall quantum wires at shallow mesa stripes is insensitive to small undulations of the mesa sidewall. For larger misalignment the surface profile continuously changes to that of the concave slow-growing sidewall along the perpendicular [2-3-3] direction, which is confirmed by spatially resolved cathodoluminescence spectroscopy. In contrast, on reactive ion etched vertical sidewalls oriented along [01-1] almost no growth occurs while the evolution of the fast-growing sidewall returns for increasing misalignment. This complicated growth behavior is related to the atomic configuration of the starting side facets after etching, which is characterized in first order by the tilt of the Ga-As tetrahedron of the bulk structure with respect to the (100) and (111) planes. The reduced growth selectivity at tilted mesa sidewalls is directly applied to the formation of coupled wire-dot arrays along zigzag patterns etched to a depth of 15 nm.

## ACKNOWLEDGMENTS

The authors thank E. Wiebicke for sample preparation and A. Trampert for cutting the grown structures. This work was supported in part by the Bundesministerium für Bildung Wissenschaft Forschung und Technologie.

<sup>1</sup>E. Kapon, D. M. Hwang, and R. Bhat, *Phys. Rev. Lett.* **63**, 430 (1989).

<sup>2</sup>X. L. Wang, M. Ogura, and H. Matsuhata, *J. Cryst. Growth* **171**, 341 (1997).

<sup>3</sup>M. Walther, T. Röhr, G. Böhm, G. Tränkle, and G. Weimann, *J. Cryst. Growth* **127**, 1045 (1993).

- <sup>4</sup>K. C. Rajkumar, A. Madhukar, K. Rammohan, D. H. Rich, P. Chen, and L. Chen, *Appl. Phys. Lett.* **63**, 2905 (1993).
- <sup>5</sup>S. Tsukamoto, Y. Nagamune, M. Nishioka, and Y. Arakawa, *Appl. Phys. Lett.* **63**, 355 (1993).
- <sup>6</sup>S. Koshiba, H. Noge, H. Akiyama, T. Inoshita, Y. Nakamura, A. Shimizu, Y. Nagamune, M. Tsuchiya, H. Sakaki, and K. Wada, *Appl. Phys. Lett.* **64**, 363 (1994).
- <sup>7</sup>H. Fujikura and H. Hasegawa, *J. Cryst. Growth* **150**, 327 (1995).
- <sup>8</sup>J. Christen, M. Grundmann, E. Kapon, E. Colas, D. M. Hwang, and D. Bimberg, *Appl. Phys. Lett.* **61**, 67 (1992).
- <sup>9</sup>M. Kihara, H. Fujikura, and H. Hasegawa, *Appl. Surf. Sci.* **117/118**, 695 (1997).
- <sup>10</sup>R. Nötzel, Z. C. Niu, M. Ramsteiner, H.-P. Schönherr, A. Trampert, L. Däweritz, and K. H. Ploog, *Nature (London)* **392**, 56 (1998).
- <sup>11</sup>R. Nötzel, U. Jahn, Z. C. Niu, A. Trampert, J. Fricke, H.-P. Schönherr, T. Kurth, D. Heitmann, L. Däweritz, and K. H. Ploog, *Appl. Phys. Lett.* **72**, 2002 (1998).
- <sup>12</sup>R. Nötzel, M. Ramsteiner, J. Menninger, A. Trampert, H.-P. Schönherr, L. Däweritz, and K. H. Ploog, *J. Appl. Phys.* **80**, 4108 (1996).
- <sup>13</sup>Z. C. Niu, R. Nötzel, U. Jahn, M. Ramsteiner, H.-P. Schönherr, J. Fricke, Z. B. Xiao, L. Däweritz, and K. H. Ploog, *Appl. Phys. A: Mater. Sci. Process.* **67A**, 135 (1998).
- <sup>14</sup>A. Richter, G. Behme, M. Süptitz, Ch. Lienau, T. Elsaesser, M. Ramsteiner, R. Nötzel, and K. H. Ploog, *Phys. Rev. Lett.* **79**, 2145 (1997).
- <sup>15</sup>R. Nötzel, L. Däweritz, and K. Ploog, *Phys. Rev. B* **46**, 4736 (1992).
- <sup>16</sup>M. Dilger, R. J. Haug, K. Eberl, A. Kurtenbach, Y. Kershaw, and K. v. Klitzing, *Appl. Phys. Lett.* **68**, 3132 (1996).
- <sup>17</sup>K. Kumakura, J. Motohisha, and T. Fukui, *J. Cryst. Growth* **170**, 700 (1997).